Progress In Electromagnetics Research C, Vol. 26, 13–27, 2012

A COMPACT ULTRAWIDEBAND MONOPOLE ANTENNA WITH 5.5 GHZ NOTCHED BAND

P. Moeikham, C. Mahatthanajatuphat, and P. Akkaraekthalin*

Department of Electrical Engineering, Faculty of Engineering, King Mongkut's University of Technology North Bangkok, Thailand

Abstract—This paper proposes a compact ultrawideband monopole antenna fed by CPW with a 5.5 GHz notched band of WLAN/WiMAX systems. The antenna input section is designed by using a gradual curvature central line and ground planes for ultrawideband achievement. In order to reject the unwanted frequency of the existing WLAN/WiMAX band, the C-shaped slit with perimeter length of a half wavelength at center frequency of 5.5 GHz has been embedded into the monopole patch. The designed antenna is completely implemented and measured for impedance bandwidth covering UWB range and stably performs omnidirectional pattern in xz plane from 3.1 to 10 GHz. The proposed antenna could potentially minimize frequency interference in the WLAN/WiMAX bands.

1. INTRODUCTION

In 2002, the Federal Communications Commission (FCC) allocated the ultrawideband (UWB) frequency range from 3.1–10.6 GHz for unlicensed UWB applications. The limitation of EIRP in band emission does not exceed -41.3 dBm/MHz for extremely wide impedance bandwidth. Printed planar monopole antennas have been designed to operate in UWB systems [1–6]. There are some wireless communication applications which have already occupied frequencies in the UWB band such as the wireless local area network (WLAN) IEEE802.11a and HIPERLAN/2 WLAN which operate at 5.15–5.35 GHz and 5.725–5.825 GHz, respectively. In addition, the worldwide interoperability for microwave access (WiMAX) has also

Received 16 September 2011, Accepted 25 November 2011, Scheduled 6 December 2011
* Corresponding author: Prayoot Akkaraekthalin (prayoot@kmutnb.ac.th).

operated covering the frequency from 5.25–5.85 GHz in some countries. In order to minimize electromagnetic interference, the stop-band filter of 5–6 GHz is often required for UWB operating systems. However, the UWB systems with additional filter circuits are more complicated and expensive. To remedy this problem, the UWB antenna with build-in frequency notch structure is often chosen. Many techniques have been employed for frequency rejection in UWB antenna designs including using radiating patches with embedded narrow slits of a half wavelength [7–10]. However, in order to achieve monopole antenna designing, a large ground plane is required, which could not be suitable for compact wireless devices. Some techniques are used to reject undesired frequencies, for examples, placing the parasitic strips on the opposite side of the radiating element [11], inserting two strips in the printed slot antenna to create two rejection bands [12], and embedding a C-shaped slit into the fed element with a parasitic strip in slot antenna [13]. However, these antennas require two metallic sides of substrates and microstrip feed lines which may be improper to use with other circuits. In [14], the band-notched slot antennas were studied, in which two types of narrow slits on the exciting stubs were used for two antennas, and two parasitic strips were placed in the rectangular slot for another one. Although, the antenna design is capable of undesired frequency rejection, the parasitic strips lead to more complex structure. In [15, 16], the band-notched antennas were designed by using resonators with embedded narrow slits into the patches, in which the former used a small strip in the notched patch and the latter used a defected ground plane. However, the antennas have more complicated structures to implement than others. In [17, 18], the frequency rejection was designed by using embedded narrow slits into ground planes. Although the antennas have good operation, some via holes may be required when connecting with other microwave circuits. The other techniques were employed to reject undesired frequencies for the planar monopole antennas including the inductively coupled resonators [19] and quarter wavelength resonators [20]. However, the former is not compact, and the latter is designed with double metallic sides on the substrate leading to more complicated structures.

This paper presents a compact UWB monopole antenna with a notched band of 5.1 to 5.9 GHz for rejecting interferences of WLAN/WiMAX operations. The proposed antenna is designed by embedding an isolated narrow slit into a radiating patch and using a CPW as feed line. The proposed antenna has compact size with its length of a half wavelength and the width of $0.3\lambda_g$ of the lowest operating frequency. Furthermore, the proposed antenna is inexpensive due to the use of low cost FR4 epoxy substrate with simple fabrication.

The details of concept design, implementation, and measurement results are presented as follows.

2. THE PROPOSED UWB MONOPOLE ANTENNA

This section presents the proposed UWB monopole antenna design. The IE3D software of Zeland is employed for simulation and optimization. The proposed antenna is designed on FR4 substrate with a thickness of 1.6 mm, relative permittivity of 4.4 and loss tangent of 0.02. Fig. 1(a) describes geometry and configuration of the UWB monopole antenna. The antenna structure consists of rectangular patch attached with flare CPW feed line. The gradual curvature central line and ground planes are employed to design the CPW feed element, as shown in Fig. 1(a). The CPW feed line is designed with characteristic impedance of 50 ohms according to the width (w) of 3.4 mm and gap distance (g) of 0.4 mm. Obviously, the gradual curvature structure of wave guide transmission line has characteristic of gradual transition guided wave to radiated wave which provides very wide bandwidth. Therefore, the gradual curvatures of both feed element and ground planes of the proposed antenna can provide extremely wide impedance bandwidth. In addition, the input impedance matching is improved by placing two small slot stubs at the central line of CPW.

There are some parameters which strongly affect its impedance characteristic, such as the height of ground plane (h_g), overall length of the antenna (h), and position of slot stubs (h_s) on feed line. These parameters will be investigated and discussed as follows. Figs. 1(b)–(d) illustrate the return losses when varying h_g, h, and h_s, respectively. It is found that varying h_g parameter mostly affects return losses of the proposed UWB monopole antenna. Fig. 1(b) displays the return loss simulated results of the h_g parameter investigation. The other parameters are fixed while h_g parameter is varied from 19.05 to 22.05 mm. The results show that the resonant frequencies are about 3, 5, 7, and 9 GHz, respectively. It can be observed that the return loss levels at the first three resonant frequencies alter as h_g increased due to the coupling effect between radiating patch and ground plane, whereas the fourth resonant frequency is shifted to lower frequencies, resulting in increasing electromagnetic coupling effect between the gradual curvature central line and ground planes. As a result, the optimal parameter of $h_g = 20.55$ mm is provided to proper return losses for the entire UWB frequency range.

The overall length of the UWB monopole antenna (h) is now studied. The other parameters of $h_g = 20.55$ mm, $h_s = 15.28$ mm,

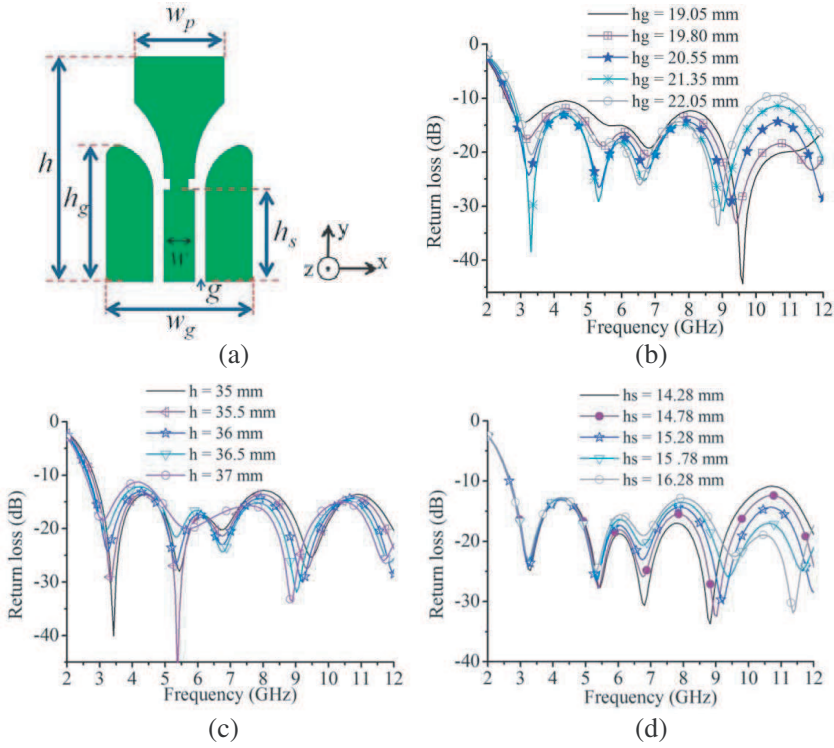

Figure 1. (a) Configuration of the proposed UWB antenna, (b) simulated results as varying h_g, (c) simulated results as varying h, and (d) simulated results as varying h_s.

$w_p = 12.86\,\text{mm}$, $w = 3.4\,\text{mm}$, $g = 0.4\,\text{mm}$ and $w_g = 19.22\,\text{mm}$ are fixed while the h parameter is investigated by adjusting the top edge of the patch from 35 to 37 mm. Fig. 1(c) depicts the simulated results of return losses as varying the parameter of h. It has been clearly found that when h parameter is increased, the first and fourth resonant frequencies are evidently moved to lower frequencies, resulting in extending electrical length of radiating patch, while it slightly affects other frequencies. In addition, with the increasing of h parameter, the higher return losses occur at the first resonant frequencies whereas the lower return losses are found at the fourth resonant frequencies due to the coupling effect between radiating patch and ground plane. Clearly, the lowest edge frequency is controlled by its length (h) which relates to a half guide wavelength response of conventional monopole antenna. The proper length h of the UWB monopole antenna is 36 mm which is

suitable for providing impedance bandwidth to cover UWB frequency range.

The slot stub position (h_s) on the central line of CPW is investigated. The h_s parameter is varied from 14.28 to 16.28 mm while other parameters are fixed. The simulated return loss results of h_s are investigated as shown in Fig. 1(d). The dimensions of slot stub with the length of 1 mm and width of 0.4 mm are obtained by empirical practice with simulation software. The results show that the input matching is worse at the 2nd, 3rd, and 4th resonant frequencies as h_s parameter is increased, and slightly affects the first resonant frequency. In addition, the 4th resonant frequency is moved to higher frequencies when the h_s parameter is increased. Clearly, the h_s parameter has affected impedance matching at the frequencies higher than 5 GHz. The h_s parameter of 15.28 mm appropriately provides a good matching at entire UWB frequency range.

The overall optimal dimensions of the UWB monopole antenna are obtained including $h = 36$ mm, $h_g = 20.55$ mm, $h_s = 15.28$ mm, $w_p = 12.86$ mm, $w = 3.4$ mm, $g = 0.4$ mm and $w_g = 19.22$ mm. Also, the slot stubs with the optimal length of 1 mm and width of 0.4 mm have been obtained. All parameters are employed to fabricate the UWB monopole antenna prototype with chemical etching on FR4 substrate with thickness of 1.6 mm, relative permittivity of 4.4 and loss tangent of 0.02, as shown in Fig. 2(a). The return loss results from simulation and measurement are compared as illustrated in Fig. 2(b). It can be clearly seen that at the frequency range from 2.78 to 8 GHz, the simulated and measured return loss results are in good agreement, while the measured results are degraded at frequencies over 8 GHz owing to increasing the losses in substrate as higher frequencies.

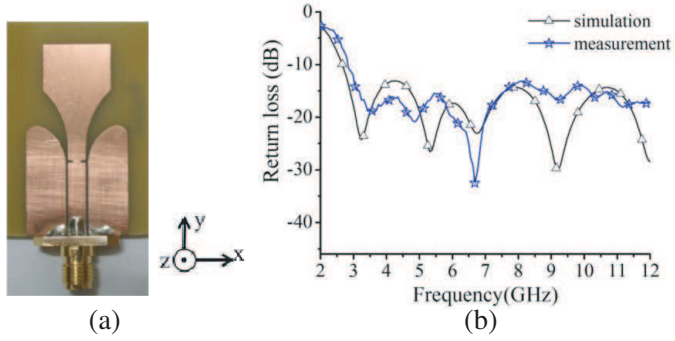

Figure 2. (a) UWB prototype antenna and (b) comparison of simulated and measured results.

Furthermore, the relative permittivity of substrate is not isotropic for the entire UWB frequency range causing poor response at high frequency. Although the discrepancy of return loss level occurs at frequencies higher than 8 GHz, the impedance bandwidth of the UWB monopole antenna still covers the UWB frequency range.

3. THE PROPOSED UWB ANTENNA WITH A NOTCHED BAND

Obviously, the UWB antenna with notched frequency band is required for reducing electromagnetic interference from the existing wireless communication systems. This section presents the proposed UWB monopole antenna with a notched band at 5.5 GHz. Fig. 3 illustrates its geometry and dimensions. The isolated narrow C-shaped slit is embedded into the metallic patch for frequencies rejection. The embedded C-shaped slit is placed symmetrically at center of the patch, and its position on the patch is denoted by h_c parameter. The C-shaped slit perimeter is determined to be approximately a half wavelength of the center rejected frequency of 5.5 GHz directly corresponding to (1). Consequently, the perimeter of C-shaped slit is about 16.59 mm at the frequency of 5.5 GHz. It is seen that the perimeter of C-shaped slit is related to its dimensions including $b = 5.54$ mm, $a = 3.57$ mm, $b' = 6.92$ mm, and $a' = 4.25$ mm. The C-shaped slit design is based on isolated up-circle and finally modified to up-ellipse structure with the widest slit of 0.69 mm $((b' - b)/2)$ and the narrowest of 0.34 mm $((a' - a)/2)$. Furthermore, after the embedded C-shaped slit is designed, it has been found that its impedance

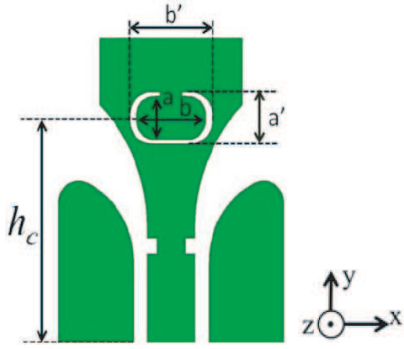

Figure 3. Configuration of the UWB monopole antenna with a C-shaped slit.

characteristics still respond to ultrawideband operation. As mentioned, the C-shaped slit perimeter is calculated from (1) where the rejected-frequency is denoted by f_{notch}, the relative permittivity of substrate by ε_r, and wavelength of frequency rejected by λ.

$$f_{\text{notch}} = \frac{3 \times 10^8}{\lambda \sqrt{\frac{\varepsilon_r + 1}{2}}} \quad \text{GHz} \tag{1}$$

Clearly, the rejected frequency is controlled by C-shaped slit perimeter. Therefore, the resulting rejected frequency from various C-shaped slit perimeters is then investigated. The other parameters are fixed whereas the C-shaped slit perimeter is adjusted by varying the b' and b parameters. The simulation results of C-shaped slit parameter studies are shown in Fig. 4.

In the first case, b' and b are simultaneously extended directly

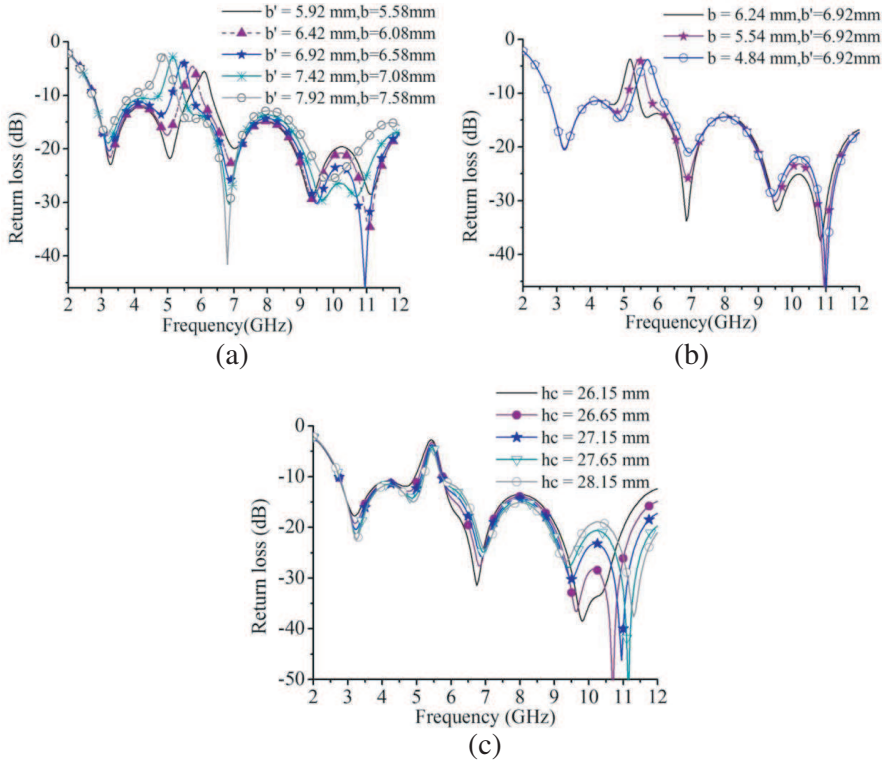

Figure 4. Simulation results of parameter studies (a) varying b and b' parameters simultaneously, (b) varying only b parameter and (c) varying h_c parameter.

corresponding to C-shaped slit perimeter increment and vice versa. b' and b parameters are varied from 5.92 to 7.92 mm and 5.58 to 7.58 mm, respectively. The simulated return losses are shown in Fig. 4(a). It can be seen that the center rejected frequency is shifted to lower frequencies due to increasing electrical length in the slit according to (1). The proper values of b' and b are 6.92 mm and 6.58 mm, respectively. It has been found that the rejected frequency is acutely changed by simultaneous controlling b' and b parameters. In addition, the only b parameter is slightly varied to fine tune the rejected frequency and bandwidth. The simulated return loss of varying only b parameter is shown in Fig. 4(b). It is observed that while b parameter is decreased, the rejected frequency is shifted to higher frequencies, and the notched bandwidth is slightly increased. The appropriate b parameter is 5.54 mm providing the rejected frequency range from 5.1 to 5.9 GHz.

The height position of C-shaped slit on patch is denoted by h_c parameter which moderately affects return loss, as shown in Fig. 4(c). It is found that the h_c parameter directly affects the notched bandwidth. On the other hand, the frequency rejection bandwidth is controlled by h_c parameter. It can be observed that when the C-shaped slit is moved down close to the curvatured border of the central feed line, the rejected-frequency bandwidth is increased. Otherwise, placing C-shaped slit deep into the patch or increasing h_c, the decrement of rejected-frequency bandwidth is obtained. The appropriate h_c parameter is 27.15 mm providing the rejected-frequency bandwidth covering from 5.1 to 5.9 GHz.

Obviously, the undesired frequency rejection band of 5.1 to 5.9 GHz is achieved by embedding C-shaped slit into the patch while the other frequencies in UWB are little affected. The mechanism of frequency rejection could be illustrated and discussed using current distributions along the radiating element. Figs. 5(a) and (c) are the cases of wave radiation at frequencies of 3.1 GHz and 7 GHz, respectively. It is seen that the current concentrates along curved edges and two sides of patch. As a result, the antenna can achieve radiate wave at those frequencies. Fig. 5(b) is the case of rejected frequency at 5.5 GHz. It can be observed that the current only concentrates around C-shaped slit and strongly concentrates at the small gap on the top C-shaped slit. There is no current distribution at the other parts of patch. This operational antenna can be considered as transmission line as the mode published and postulated in [7, 9]. For more clear consideration, the enlargement of current distribution on C-shaped slit and the equivalent circuit model at rejected frequency are depicted in Figs. 6(a) and (b), respectively. At the frequency of 5.5 GHz, the narrow slit acts as series element in transmission line, while the current

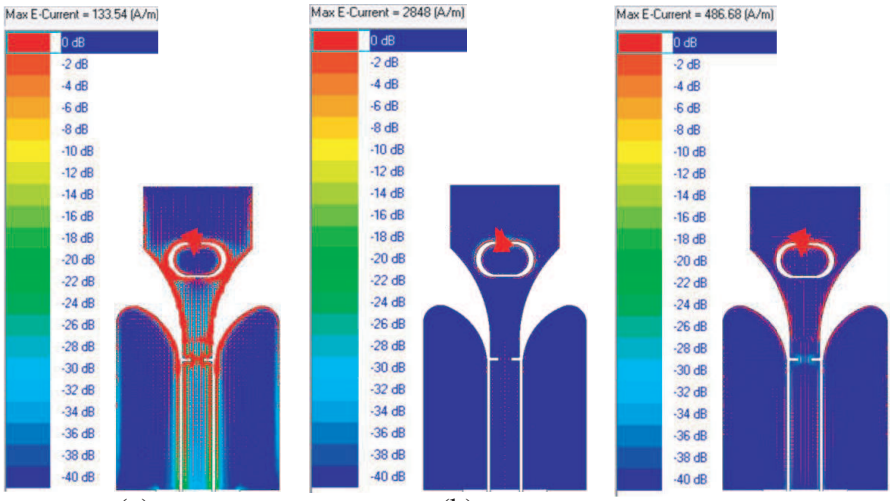

Figure 5. Current distributions at (a) 3.1 GHz, (b) 5.5 GHz, and (c) 7 GHz.

distributes around narrow slit with strong concentration at the gap on the top of C-shaped slit acting as short circuit. As a result, the impedance on the top of C-shaped slit is nearly zero and on the bottom is nearly high impedance. Therefore, the impedance nearby feed point acutely changes and the high return loss at that frequency is occurred. The antenna could not radiate wave and the frequency rejection is achieved.

Figure 7(a) shows prototype of the proposed antenna which is implemented on FR4 epoxy substrate with thickness of 1.6 mm, relative permittivity of 4.4 and loss tangent of 0.02. The prototype antenna is terminated with SMA connector for the measurement purpose. Fig. 7(b) illustrates the comparison of the measured and simulated return loss results. The measurement and simulation results are shown in solid line with star and solid line with circle symbols, respectively. The results show that the frequency notched band of measured and simulated results are in good agreement. At the frequency over 6 GHz, both results of measurement and simulation are in fair agreement. The impedance bandwidth of measured result covers frequency range from 2.85 GHz to exceed 12 GHz and notched frequency range from 5.1 to 5.9 GHz. Although, the discrepancy of return loss at frequency over 6 GHz is found, the proposed antenna provides impedance bandwidth covering ultrawideband frequency range. The degraded response of

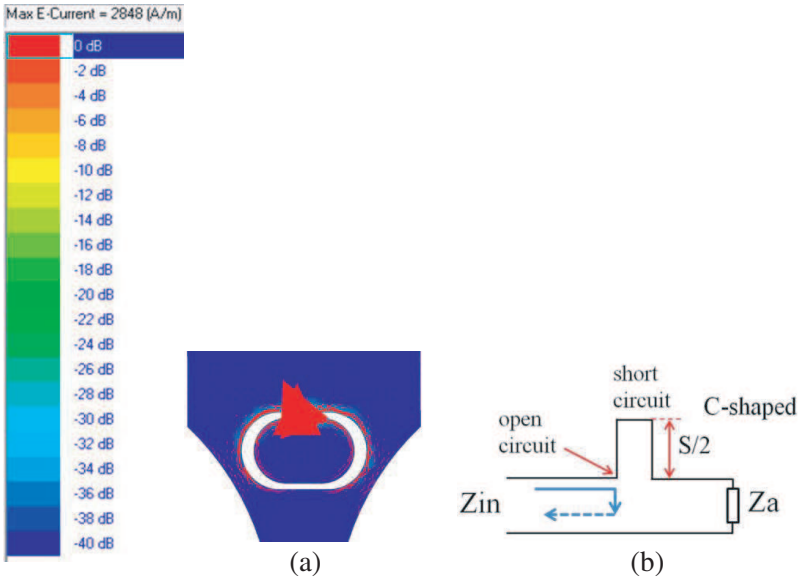

Figure 6. (a) Enlargement of current around C-shaped slit and (b) equivalent circuit model for the antenna with C-shaped slit at the frequency of 5.5 GHz.

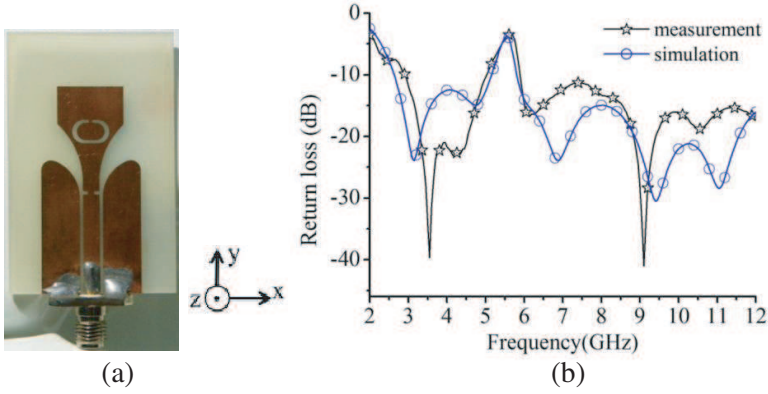

Figure 7. (a) The proposed antenna prototype and (b) comparison of return losses from measured and simulated results.

substrate at high frequency is a major cause of discrepant measurement results. In addition, the implementation tolerance and SMA alignment with central feed line or the gap between the SMA and terminated

point cause degrade measurement results of the prototype antenna.

The radiation patterns of the proposed antenna in xz and yz planes are shown in Figs. 8(a)–(d) and Figs. 8(e)–(h), respectively. It is found that the co-polarization measurement radiation patterns of the proposed antenna show good agreement with simulation results at all frequencies in xz plane, as shown in Figs. 8(a)–(d). A little discrepancy between the measurement and simulation results occurs at the frequency of 10 GHz. Moreover, at the frequencies of 9 GHz and 10 GHz, the high cross-polarization levels increase due to the major curvature parts at higher frequencies. Although there is a little distort in the radiation pattern, the radiation patterns are still omnidirectional at the entire UWB frequency range in xz plane.

The radiation patterns of the proposed antenna in yz plane are shown in Figs. 8(e)–(h) at frequencies of 3.1, 7, 9, and 10 GHz, respectively. It is found that the co-polarization measurement radiation patterns of the proposed antenna show good agreement with simulation results at frequencies of 3.1, 7, and 9 GHz. At the frequency of 10 GHz, the radiated distortion occurs at the angle of 200 to 350 degrees. The higher mode operation of the antenna causes the discrepancies. Although a little distortion of radiation patterns occurs, the proposed antenna provides bi-directional radiation patterns at all frequencies in yz plane. In addition, the polarization of the proposed antenna is linear.

Figure 9(a) displays the comparison of maximum gains between measurement and simulation results of the proposed antenna. It can be observed that the gain sharply decreases at rejected frequency range from 5 to 6 GHz due to embedded C-shaped slit with its length corresponding to a half wavelength of center rejected frequency band of 5.5 GHz. The measured maximum gain is about 4.5 dBi while the simulated gain is 3.4 dBi at frequency of 7.5 GHz. Although there are some differences between measured and simulation gain results, their tendencies are similar.

The impulse response is an important characteristic of the UWB antenna. The small group delay time or linear phase response of the UWB antenna shows a good impulse response. Fig. 9(b) depicts group delay time and phase response measured results of the proposed antenna. The results show that the group delay time does not exceed 9.5 ns, and the average delay time is about 2 ns. Furthermore, the proposed antenna has a compact size which can be properly applied to USB applications.

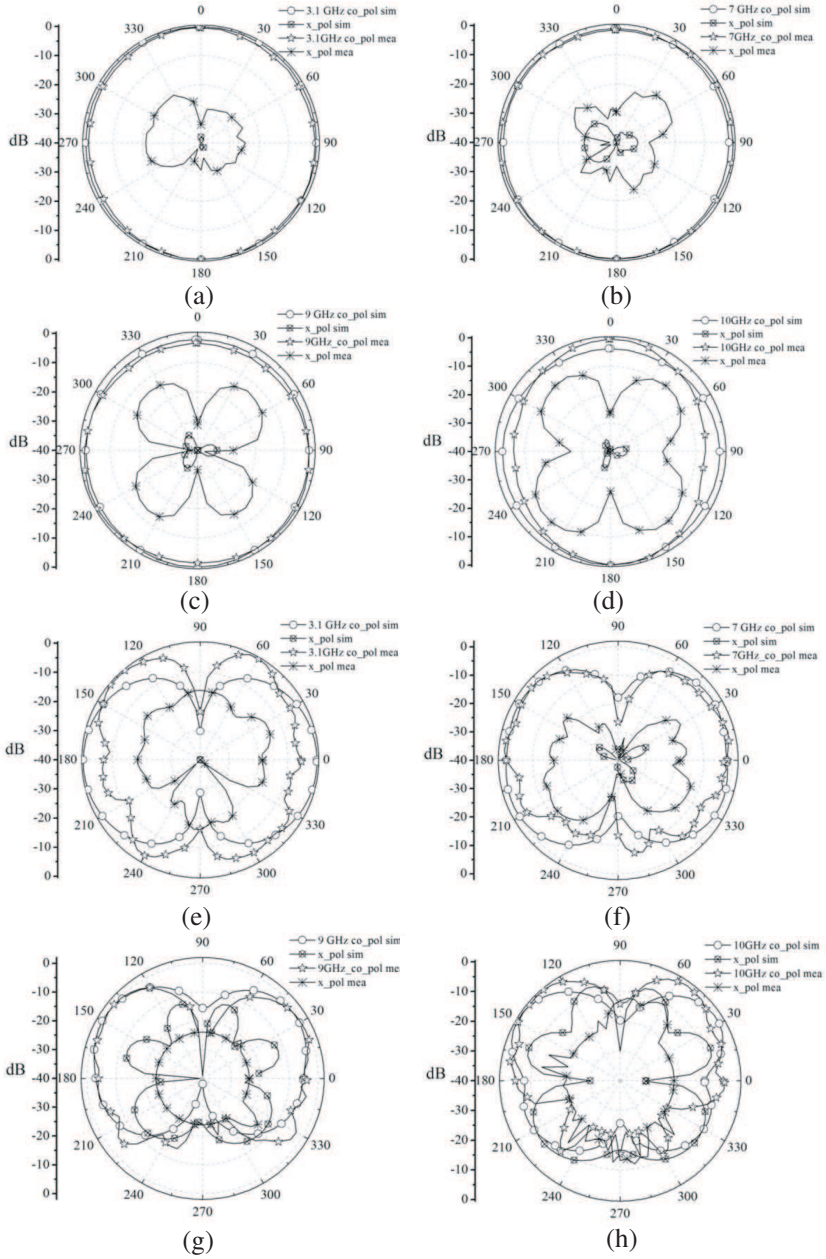

Figure 8. Radiation patterns at (a) 3.1 GHz, (b) 7 GHz, (c) 9 GHz, (d) 10 GHz in xz plane and (e) 3.1 GHz, (f) 7 GHz, (g) 9 GHz, and (h) 10 GHz in yz plane.

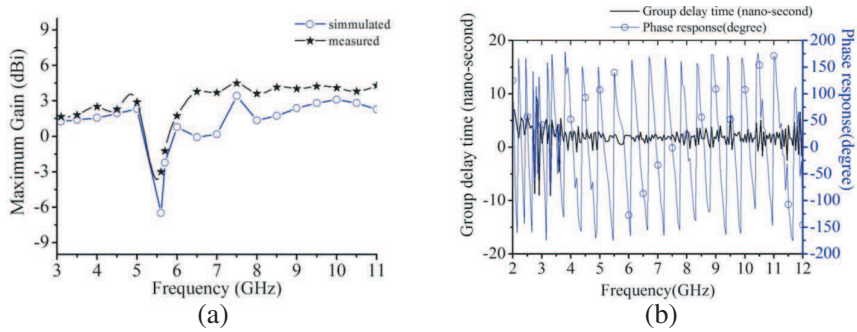

Figure 9. (a) Comparison of measured and simulated maximum gain results and (b) time domain of the proposed antenna.

4. CONCLUSION

The proposed antenna has impedance bandwidth covering UWB range and radiation bandwidth from 3.1 to 10 GHz. The antenna provides a nearly omnidirectional radiation pattern in xz plane and likely bi-direction pattern in yz plane at the frequencies from 3.1 to 10 GHz. By embedding C-shaped slit with the perimeter length about $\lambda/2$ at center frequency band of 5.5 GHz into the patch at appropriate location, the band rejected frequency range from 5 to 6 GHz is obtained. Therefore, the proposed antenna has a potential to reject electromagnetic interference in WLAN/WiMAX operation frequency of 5.5 GHz band. Furthermore, the proposed antenna has a compact size about thumb drive which is proper applied for USB applications.

ACKNOWLEDGMENT

The authors would like to thank the Repair and Calibration Sector TOT Innovation Institute of Thailand and the Telecommunication Laboratory of Engineering Faculty, Rajamangala University of Technology Krungthep (RMUTK) for antenna measurement.

REFERENCES

1. Ma, T.-G. and C.-H. Tseng, "An ultrawideband coplanar waveguide-fed tapered ring slot antenna," *IEEE Trans. on Antennas and Propag.*, Vol. 54, 1105–1110, Apr. 2006.

2. Wong, K.-L., C.-H. Wu, and S.-W. Su, "Ultrawide-band square planar metal plate monopole antenna with a trident-shaped feeding strip," *IEEE Trans. on Antennas and Propag.*, Vol. 53, 1262–1269, Apr. 2005.
3. Jafari, H. M., M. J. Deen, S. Hranilovic, and N. K. Nikolova, "A study of ultrawideband antennas for near-field imaging," *IEEE Trans. on Antennas and Propag.*, Vol. 55, 1184–1188, Apr. 2007.
4. Chu, Q.-X. and Y.-Y. Yang, "A compact ultrawideband antenna with 3.4/5.5 GHz dual band-notched characteristics," *IEEE Trans. on Antennas and Propag.*, Vol. 56, 3637–3644, Dec. 2008.
5. Liang, J. X., C. C. Chiau, X. D. Chen, and C. G. Parini, "Study of a printed circular disc monopole antenna for UWB systems," *IEEE Trans. on Antennas and Propag.*, Vol. 53, 3500–3504, Nov. 2005.
6. Liang, X.-L., S.-S. Zhong, and F.-W. Yao, "Compact UWB tapered CPW-fed planar monopole antenna," *Proc. APMC 2005 Int. Conf.*, 2005.
7. Lee, W.-S., D.-Z. Kim, K.-J. Kim, and J.-W. Yu, "Wideband planar monopole antennas with dual band-notched characteristics," *IEEE Trans. on Microwave Theory and Techniques*, Vol. 54, 2800–2806, Jun. 2006.
8. Zhang, Y., W. Hong, C. Yu, Z.-Q. Kuai, Y.-D. Don, and J.-Y. Zhou, "Planar ultrawideband antennas with multiple notched bands based on etched slots on the patch and/or split ring resonators on the feed line," *IEEE Trans. on Antennas and Propag.*, Vol. 56, 3063–3068, 2008.
9. Chu, Q.-X. and Y.-Y. Yang, "A compact ultrawideband antenna with 3.4/5.5 GHz dual band-notched characteristics," *IEEE Trans. on Antennas and Propag.*, Vol. 56, 3637–3644, Dec. 2008.
10. Liu, H.-W., C.-H. Ku, and C.-F. Yang, "Novel CPW-fed planar monopole antenna for WiMAX/WLAN applications," *IEEE Antennas Wireless Propag. Lett.*, Vol. 9, 240–243, 2010.
11. Zhang, M., Y.-Z. Yin, J. Ma, Y. Wang, W.-C. Xiao, and X.-J. Liu, "A racket-shaped slot UWB antenna coupled with parasitic strips for band-notched application," *Progress In Electromagnetics Research Letters*, Vol. 16, 35–44, 2010.
12. Chen, W.-S. and K.-Y. Ku, "Band-rejected design of the printed open slot antenna for WLAN/WiMAX operation," *IEEE Trans. on Antennas and Propag.*, Vol. 56, 1163–1169, Apr. 2008.
13. Gao, G.-P., Z.-L. Mei, and B.-N. Li, "Novel circular slot UWB antenna with dual band-notched characteristics," *Progress In*

Electromagnetics Research C, Vol. 15, 49-63, 2010.

14. Lin, Y.-C. and K.-J. Hung, "Compact ultrawideband rectangular aperture antenna and band-notched designs," *IEEE Trans. on Antennas and Propag.*, Vol. 54, 3075–3081, Nov. 2006.
15. Ren, L.-S., F. Li, J.-J. Zhao, G. Zhao, and Y.-C. Jiao, "A novel compact UWB antenna with 3.5/5.2/5.8 GHz triple band-notched characteristics," *Progress In Electromagnetics Research Letters*, Vol. 16, 131–139, 2010.
16. Li, W. T., X. W. Shi, and Y. Q. Hei, "Novel planar UWB monopole antenna with triple band-notched characteristics," *IEEE Antennas Wireless Propag. Lett.*, Vol. 8, 1094–1098, 2009.
17. Yang, Y.-B., F.-S. Zhang, F. Zhang, L. Zhang, and Y.-C. Jiao, "Design of novel wideband monopole antenna with a tunable notched-band for 2.4 GHz WLAN and UWB applications," *Progress In Electromagnetics Research Letters*, Vol. 13, 93–102, 2010.
18. Tseng, C.-F. and C.-H. Hsu, "Design of planar UWB dipole antenna with band-notched characteristics," *Progress In Electromagnetics Research C*, Vol. 11, 1–10, 2009.
19. Ma, T.-G. and J.-W. Tsa, "Band-rejected ultrawideband planar monopole antenna high frequency selectivity and controllable bandwidth using inductively coupled resonator pairs," *IEEE Trans. on Antennas and Propag.*, Vol. 58, 2747–2752, Aug. 2010.
20. Kim, D.-Z., W.-I. Son, W.-G. Lim, H.-L. Lee, and J.-W. Yu, "Integrated planar monopole antenna with microstrip resonators having band notched characteristics," *IEEE Trans. on Antennas and Propag.*, Vol. 58, 2837–2842, Sep. 2010.